Contributions to Geophysics and Geodesy Vol. 46/2, 2016 (91–109)

Tectonic classification of vertical crustal motions – a case study for New Zealand

Robert TENZER[1,2,*], Ali FADIL[3]

[1] NTIS – New Technologies for the Information Society, Faculty of Applied Sciences, University of West Bohemia, Plzeň, Czech Republic

[2] The Key Laboratory of Geospace Environment and Geodesy, School of Geodesy and Geomatics, Wuhan University,
129 Luoyu Road, Wuhan, 430079, China;
phone: +86 27 6877 8649; fax: +86 27 6877 1695; e-mail: rtenzer@sgg.whu.edu.cn

[3] National School of Surveying, Faculty of Sciences, University of Otago,
310 Castle Street, Dunedin, New Zealand

Abstract: We investigate the relationship between vertical crustal motion and tectonic block configuration. The study is conducted along the active tectonic margin between the Australian and Pacific tectonic plates in New Zealand with a well-defined tectonic block configuration. For this purpose, the rates of vertical crustal motions relative to the ITRF2008 reference frame are estimated based on processing the GPS data (provided by the GeoNET project) collected at 123 continuous and semi-continuous GPS sites. The numerical results confirmed the uplift of the central Southern Alps at the current rate of 4.5 mm/yr. This tectonic uplift is coupled in the South Island by the subsidence on both sides of the Southern Alps. The detected rates of subsidence in the eastern South Island are typically less than 1 mm/yr. The subsidence in the Buller Region (in the northwest South Island) is 1.4–1.5 mm/yr. Except for the Taupo Volcanic Zone and the upper Raukumara Block (in the central and northeast North Island), the subsidence is prevailing in the North Island. The systematic subsidence up to 9 mm/yr is detected along the Dextral Fault Belt (in the lower North Island). The largest localized vertical displacements (between −10 and 17 mm/yr) in the Taupo Volcanic Zone are attributed to active tectonics, volcanisms and geothermal processes in this region. A classification of these vertical tectonic motions with respect to the tectonic block configuration reveals that most of tectonic blocks are systematically uplifted, subsided or tilted, except for regions characterized by a complex pattern of vertical motions attributed to active geothermal and volcanic processes.

Key words: GPS, tectonic setup, vertical crustal motion, volcanism

*corresponding author

doi: 10.1515/congeo-2016-0007

1. Introduction

The horizontal tectonic motions in New Zealand were studied extensively by *Bourne et al. (1998)*, *Beavan et al. (1999; 2002; 2007)*, *Beavan and Blick (2005)*, *Wallace et al. (2007)*, and others. *Beavan and Haines (2001)* produced the present-day horizontal velocity and strain rate fields of the Pacific-Australian plate boundary zone throughout New Zealand. These data were used to compile the horizontal deformation model which is utilized in the definition of the (semi-dynamic) New Zealand Geodetic Datum 2000 – NZGD2000 (*Blick et al., 2003*). The limiting aspects of the NZGD2000 deformation model were outlined by *Beavan and Blick (2005)*.

Except for the designated areas of significant geophysical interest in the Taupo Volcanic Zone and transect across the central Southern Alps, no systematic studies of vertical motions in New Zealand were conducted until recently. *Tenzer et al. (2012)* used GPS data from GeoNET[1] continuous and semi-continuous sites to estimate (relative) rates of vertical motions in New Zealand. Their solution was obtained from a regional analysis using Bernese v5.0 software (*Dach et al., 2007*) with fixed orbits in the ITRF2000/IGb00 reference frame and several regional IGS stations constrained to their IGb00 positions and velocities. The daily position time series contain substantial common-mode noise that was reduced by regional filtering (*Wdowinski et al., 1997*), implemented in combination with outliers rejection as described by *Beavan (2005)*.

In this study we investigate the present-day vertical crustal deformations in New Zealand and their relationship with the regional tectonic block configuration. The existing regional studies of vertical motions in New Zealand are briefly reviewed in Section 2. The overview of New Zealand's tectonic setup is given in Section 3. The GPS processing strategy is summarized in Section 4. The results are discussed in Section 5 and concluded in Section 6.

2. Regional studies of vertical motions

2.1. Southern Alps

The Southern Alps have been subject to a significant number of surface

[1]http://www.geonet.org.nz/

deformation and geophysical studies due to their close proximity to the Pacific and Australian plate boundary (*Wellman, 1979; Bull and Cooper, 1986*). *Wellman (1979)* inferred vertical rates of up to 10 mm/yr from measurements of Quaternary faulting along the Alpine Fault and corrections for sea level changes, and from extrapolations of apparent tilting of lake shorelines. The estimates based on geochronological data (e.g. *Batt and Braun, 1999*) suggest rock exhumation rates up to 10 mm/yr. *Beavan et al. (2004)* investigated the rates of relative vertical movement across the central Southern Alps. They estimated that the highest vertical rates are about 6–7 mm/yr relative to sites located on the Pacific plate. These results were obtained with average $(1-\sigma)$ uncertainties better than 0.5 and 1 mm/yr at continuous and semi-continuous GPS sites, respectively. In a more recent study, *Beavan et al. (2010)* estimated the relative vertical rates at the profile across the Southern Alps with $(1-\sigma)$ uncertainties of 0.2–0.9 mm/yr using up to 10 years of continuous and semi-continuous GPS data. According to their estimation, the maximum rate of 5 mm/yr (relative to the east coast) occurs on either side of the crest of the Southern Alps and 20-30 km southeast of the Alpine Fault.

2.2. Taupo Volcanic Zone

The vertical deformations in the Taupo Volcanic Centre and Taupo Fault Belt have been monitored since 1979 using a portable lake levelling survey techniques (*Otway et al., 2002*). These observations have revealed complex episodic deformations that are apparently closely linked to earthquake swarms and surface faulting (*Otway, 1986; Grindley and Hull, 1986; Otway et al., 2002*). The geological evidence indicates that vertical motion in the Taupo Fault Belt appears to consist of initial aseismic uplift, followed by seismic normal faulting and then a period of aseismic subsidence (*Grindley and Hull, 1986; Otway, 1986*). *Samsonov et al. (2011)* used differential interferomeric synthetic aperture radar (DInSAR) observations collected by ALOS PALSAR during 2006–2010, and compared them with displacement observations from continuous GPS sites in the Taupo Volcanic Zone. They detected localized subsidence at Kawerau, Ohaaki and Tauhara-Wairakei geothermal regions.

3. New Zealand's tectonic setting

The tectonic setup of New Zealand is characterized by the collision of the Pacific and Australian plates. The boundary between these two plates does not have a single location (*Wallace et al., 2004; 2007*). Instead, it is a broad zone of deformation covering much of the country. The tectonic block configuration including major active fault systems in New Zealand are shown in Fig. 1.

3.1. North Island

Most of the North Island is situated along the obliquely convergent zone. Active tectonics in the North Island are dominated by subduction at the Hikurangi Trough (*Nicol et al., 2007; Nicol and Wallace, 2007*), back-arc rifting in the Taupo Volcanic Zone, and strike-slip faulting in the Dextral Fault Belt (*Wallace et al., 2004*). The inter-plate relative horizontal motions decrease in rate and takes on a greater margin-parallel component southward along the New Zealand margin (*DeMets et al., 1990; 1994*). The subduction of the oceanic Hikurangi Plateau is marked by the Hikurangi Trough (and further north by the Kermadec Trench). Plate shortening in the accretionary wedge is observed between the Hikurangi Trough and the east coast of the North Island (*Barnes and Mercier de Lepinay, 1997*). Upper plate shortening (over the last 5 Myr) was also found in the subaerial portion of the eastern North Island (*Nicol et al., 2002; Nicol and Beavan, 2003*). The Taupo Volcanic Zone has been opening for at least the last 2–4 Myr (*Cole et al., 1995*) with the estimated maximum horizontal rates of ∼20 mm/yr (*Villamor and Berryman, 2001*). The results of geological and geodetic studies indicate the rotation of the eastern North Island with the consequent extension and subaerial upper plate shortening in the North Island (e.g., *Walcott, 1984; Beanland and Haines, 1998; Beavan and Haines, 2001*). The Dextral Fault Belt has been active since at least 1 Myr (*Kelsey et al., 1995*) with the estimated strike-slip horizontal motions up to 20 mm/yr (*Beanland, 1995*). The eastern North Island (including the northern Wanganui Block) is dominated by the extensional faulting occurring on the Cape Egmont Fault Zone.

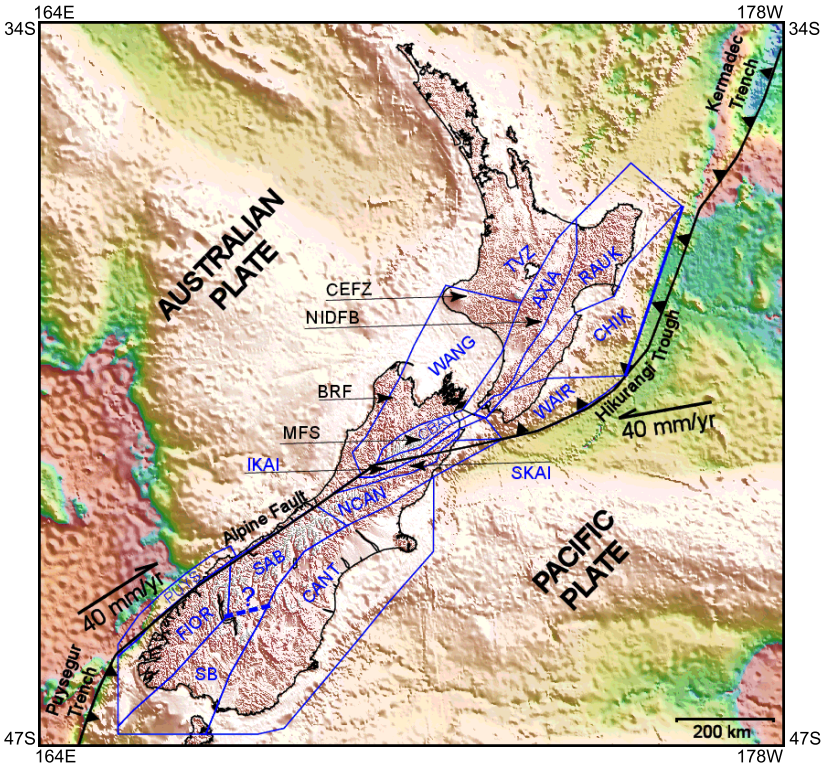

Fig. 1. Tectonic block configuration of New Zealand used in this paper. Major active fault systems are in black (from GNS's active faults database; http://data.gns.cri.nz/af) and tectonic blocks are in blue. Active fault abbreviations: MFS: Marlborough Fault System; NIDFB: North Island Dextral Fault Belt; CEFZ indicates the region where extensional faulting occurs on the Cape Egmont Fault Zone; BRF: approximate location of shortening related faults of the Buller region in the northwestern South Island. Tectonic block abbreviations: TVZ: Taupo Volcanic Zone; WANG: Wanganui Block; IXIA: Axial Ranges Block; WAIR: Wairarapa Block; CHIK: Central Hikurangi Block; RAUK: Raukumara Block; FIOR: Fiordland Block; SB: Southland Block; CANT: Canterbury/Otago Block; SAB: Southern Alps Block; NCAN: Northern Canterbury Block; IKAI: Inland Kaikoura block, SKAI: Seaward Kaikoura block; (CBAY) Cloudy Bay Block.

3.2. South Island

The subduction of the Australian plate underneath the Pacific plate is marked by the Puysegur Margin to the southwest of the South Island. Along the central South Island, these two plates are colliding by oblique strike

slip. The response to this oblique continental convergence (which started ∼20 Myr) was the formation of the Southern Alps (*Cande and Stock, 2004*). In this region the tectonic plate margin is distinctively marked by the Alpine Fault. In the northern South Island with extension to the eastern North Island, the oblique subduction is opposite with the Pacific plate forced below the Australian plate along the Hikurangi margin. The Alpine Fault is connected to the Hikurangi Subduction Zone by several dextral strike-slip faults known as the Marlborough Fault Zone. The Australia-Pacific relative plate motion, accommodated across the South Island, is estimated to be ∼39 mm/yr with a shortening component normal to the Alpine Fault of 6–9 mm/yr (*DeMets et al., 2010*; see also *Beavan et al., 2002*; *Holt and Haines, 1995*; *Beavan et al., 1999*; *Norris and Cooper, 2001*). The central segment of this fault shows an oblique-reverse displacement, with a late Quaternary slip rate of 20–30 mm/yr (e.g. *Berryman et al., 1992; Sutherland and Norris, 1995*). The Buller region in the northwest of the South Island consists of several shortening-related faults.

4. GPS data analysis

We processed GPS phase data from 123 sites provided by the GeoNet project. The range of the GPS time series varies significantly with the longest data observed from 2005 until December 2014, while the shortest time series comprised data only over the period of 3 years. The analysis of these GPS phase data was performed in a consistent way over the whole considered data span using the Precise Point Positioning (PPP) mode of GIPSY-OASIS II software (*Webb and Zumberge, 1995; Zumberge et al., 1997*) and JPL reprocessed products.

The estimated parameters include the station positions and clocks, phase biases, tropospheric delays and horizontal tropospheric gradients. The a priori zenith hydrostatic delay (ZHD) was calculated based on the station height and thus regarded as constant, while the zenith wet delay (ZWD) and the horizontal tropospheric gradient components (north and east) were modelled as Random Walk (RW) variables, and were estimated every 5 min. as time-dependent parameters (*Bar-Sever et al., 1998*). The solid Earth and pole tide corrections were treated according to the IERS Conventions 2010

(*Petit and Luzum, 2010*). The ocean-tide loading corrections were applied based on the FES2004 ocean tide model (*Lyard et al., 2006*). The antenna phase centre models (*Schmid et al., 2007*) and the Global Mapping Function (*Boehm et al., 2006*) were taken into consideration. The resulting daily solutions were aligned to the ITRF2008 reference frame (*Altamimi et al., 2011*) applying Helmert's seven-parameter transformation (JPL x-files).

Langbein and Johnson (1997), *Mao et al. (1999)*, *Williams (2003)*, and others have demonstrated that the measurement noise associated with the de-trended GPS position time-series residuals is time correlated. If these correlations are not properly accounted for, the formal errors of the GPS derived velocities are roughly underestimated by a factor of 5 to 10. First, the GPS vertical time series were inspected for possible outliers and offsets (*Herring, 2003*) due to antenna changes and/or earthquakes and/or slow slip events (e.g. *Wallace and Beavan, 2010; Kim et al., 2011*). To assign realistic uncertainties on the GPS derived velocities, we carefully examined the GPS vertical time series by a maximum likelihood method (*Williams, 2008*) that simultaneously estimates linear trends, annual periodic signal terms, power-law and white noise parameters, and offsets at specified times. In the case of clear presence of the post-seismic effect or slow slip events (at the sites: KAPT, PNUI, PYGR, TAKP) the co-seismic offset and the accumulated event motion were estimated by allowing an exponential fit to a break at the time of the event (*Herring, 2003*).

A combination of power-law plus white noise model provides the most likely stochastic description of the GPS time series, which is consistent with former studies (e.g. *Mao et al., 1999; Amiri-Simkooei et al., 2007*). The average spectral index is -0.9 ± 0.3, which is close to -1, thus indicates flicker noise. Under this assumption, the average noise levels are 3.4 ± 1.9 mm and 12.2 ± 3.8 mm/yr$^{0.25}$ for the white and power law noises respectively. The estimated rates of vertical crustal motions relative to the ITRF2008 reference frame are summarized in Table 1 (see also Fig. 2).

5. Discussion

Despite the upper and western parts of the North Island and large regions of the South Island are not sufficiently constrained by the geodetic

Table 1. Vertical velocity rates and their standard uncertainties at 123 GPS sites in New Zealand. For the abbreviations used for the GPS sites see: http://magma.geonet.org.nz /resources/network/netmap.html; Long. = Longitude, Lat. = Latitude, Veloc. = Velocity, SD = Standard Deviation.

GPS site	**Long.** [deg]	**Lat.** [deg]	**Veloc.** [mm/yr]	**SD** [mm/yr]	**GPS site**	**Long.** [deg]	**Lat.** [deg]	**Veloc.** [mm/yr]	**SD** [mm/yr]
AKTO	176.461	−40.540	−3.37	0.34	MAVL	168.118	−45.367	0.16	0.49
AUCK	174.834	−36.603	−0.83	0.43	MCNL	176.697	−39.444	−3.21	2.72
AVLN	174.933	−41.196	−0.97	0.40	MQZG	172.655	−43.703	−1.07	0.45
BHST	176.063	−39.489	−0.97	1.36	MTBL	175.536	−40.181	−3.65	0.79
BIRF	176.246	−40.680	−4.52	0.44	MTJO	170.465	−43.986	0.43	0.23
BLUF	168.292	−46.585	−0.10	0.45	NETT	170.061	−43.756	2.93	0.79
BNET	170.190	−43.863	3.69	0.46	NLSN	173.434	−41.184	−1.48	0.52
CAST	176.202	−40.910	−3.84	0.42	NMAI	176.807	−39.097	−1.24	1.23
CKID	177.076	−39.658	−0.32	1.06	NPLY	174.118	−39.183	−1.14	0.20
CLIM	175.145	−41.145	−1.98	0.47	NRRD	175.761	−40.385	−5.88	0.60
CMBL	174.214	−41.749	−0.08	0.31	OTAK	175.170	−40.817	−3.93	0.63
CNCL	169.856	−43.666	4.33	0.29	OUSD	170.511	−45.870	−0.45	0.41
CNST	178.211	−38.488	1.49	1.26	PAEK	174.952	−41.022	−1.70	0.34
CORM	175.750	−36.865	−0.60	0.37	PALI	175.255	−41.569	−4.92	0.43
DNVK	176.167	−40.299	−3.69	0.51	PARI	177.883	−38.923	−4.41	1.03
DUND	170.597	−45.884	−1.42	0.40	PARW	175.427	−41.382	−4.24	0.26
DUNT	170.629	−45.814	−0.69	0.24	PAWA	176.864	−40.033	−0.34	1.46
DURV	173.922	−40.802	−1.41	0.43	PNUI	176.200	−39.917	−9.35	0.47
GISB	177.886	−38.635	−0.08	0.73	PORA	176.635	−40.266	−2.47	0.95
GLDB	172.530	−40.827	−1.43	0.36	PTOI	175.999	−40.601	−4.16	0.42
GNBK	175.238	−40.080	−3.19	1.14	PUKE	178.257	−38.071	0.64	0.37
GRAC	174.917	−41.235	−2.34	0.46	PYGR	166.681	−46.166	0.78	0.91
GRNG	175.459	−39.976	−1.96	1.00	QUAR	169.816	−43.532	1.08	0.49
HAAS	168.786	−44.073	0.96	0.45	RAHI	177.086	−38.916	−0.94	0.75
HAMT	175.109	−37.807	−0.24	0.42	RGAR	176.343	−38.562	−3.55	0.97
HANA	177.569	−38.687	−0.13	1.66	RGCR	176.378	−38.105	−4.99	0.98
HAST	176.727	−39.617	−4.44	0.63	RGHR	176.288	−38.386	−8.72	0.99
HIKB	178.303	−37.561	0.09	0.30	RGKA	176.244	−38.020	−0.94	0.77
HOKI	170.984	−42.713	0.24	0.37	RGLI	176.386	−38.003	−3.73	0.71
HOLD	175.515	−40.897	−2.86	0.54	RGMK	176.467	−38.138	−17.11	1.06
HORN	170.105	−43.777	4.51	0.35	RGMT	176.725	−37.915	9.80	0.73
KAHU	176.876	−39.794	−1.92	0.41	RGOP	176.556	−37.846	1.76	0.85
KAIK	173.534	−42.425	−1.35	0.37	RGRE	176.521	−38.057	−3.50	0.64
KAPT	174.910	−40.861	−5.31	0.52	RGRR	176.515	−38.339	−4.79	2.22
KARA	169.775	−43.608	1.59	0.63	RGTA	176.506	−38.234	−13.35	0.72
KERE	176.370	−39.643	−5.68	0.68	RGUT	176.194	−38.177	−4.78	0.98
KOKO	177.668	−39.016	−1.07	0.68	RIPA	176.492	−39.166	−0.04	0.27
KORO	175.424	−40.409	−5.74	0.96	TAKL	174.770	−36.844	−0.22	0.46
KTIA	173.273	−35.069	−3.24	1.47	TAKP	175.963	−40.062	−8.57	0.35
LEVN	175.241	−40.589	−5.69	0.85	TAUP	176.081	−38.743	3.06	0.79
LEXA	169.308	−45.231	0.00	0.34	TEMA	175.890	−41.107	−3.99	0.61
LEYL	176.937	−39.332	−3.22	1.05	TGHR	175.712	−38.678	−0.04	0.56
LKTA	172.266	−42.783	1.20	0.27	TGOH	176.047	−38.846	−0.21	1.02
LYTT	172.722	−43.606	−0.86	0.30	TGRA	175.770	−38.863	0.53	0.80
MAHI	177.907	−39.153	−1.63	1.46	TGTK	175.811	−38.611	−0.69	0.72
MAHO	174.854	−38.513	−1.90	0.37	TGWH	175.940	−38.673	−2.77	1.02
MANG	175.575	−40.669	−3.55	0.37	THAP	175.786	−39.683	−0.95	0.93
MAST	175.585	−41.062	−3.39	0.77	TINT	175.886	−40.776	−5.78	0.45
MATW	177.526	−38.334	0.89	0.50	TORY	174.280	−41.192	0.01	0.66

Table 1. Continued from the previous page.

GPS site	Long. [deg]	Lat. [deg]	Veloc. [mm/yr]	SD [mm/yr]	GPS site	Long. [deg]	Lat. [deg]	Veloc. [mm/yr]	SD [mm/yr]
TRAV	175.688	−41.398	−4.31	0.25	VGTS	175.609	−39.277	−0.99	0.42
TRNG	176.261	−37.729	0.36	0.67	VGWH	175.589	−39.282	−0.15	0.36
UTK2	175.838	−39.746	−4.33	2.58	VGWN	175.598	−39.327	0.57	0.22
UTK3	175.836	−39.748	−3.51	1.49	WAIM	170.920	−44.656	−0.79	0.35
UTK4	175.837	−39.749	−3.81	2.06	WAKA	169.885	−43.584	2.56	0.49
VGFW	175.553	−39.255	−1.33	0.30	WANG	174.821	−39.787	−0.38	0.52
VGKR	175.641	−39.094	−1.80	0.34	WEST	171.806	−41.745	−1.51	0.36
VGMO	175.754	−39.407	0.96	0.45	WGTN	174.806	−41.323	−1.98	0.36
VGMT	175.470	−39.385	1.08	0.85	WGTT	174.782	−41.290	−3.05	0.21
VGOB	175.542	−39.200	−1.90	0.53	WHNG	174.315	−35.804	−0.41	0.33
VGOT	175.665	−39.163	−1.99	0.60	WPAW	176.543	−39.896	−7.37	0.70
VGPK	175.346	−39.289	−0.91	0.87	WPUK	176.441	−40.064	−4.52	0.86
VGTR	175.548	−39.298	−0.37	0.40					

data (continuous GPS sites), major features of vertical motions over most of New Zealand can clearly be recognized. The classification of rates of uplift/subsidence with respects to the tectonic block configuration in the North and South Islands (as shown in Fig. 1) is given in Table 2.

5.1. North Island vertical motions

As seen in Fig. 2, the systematic tectonic subsidence is dominated in the North Island. This subsidence is detected at the GPS sites located in the upper and west North Island (including the upper Wanganui Block), lower and central Raukumara Block, Axial Ranges Block, Wairarapa Block and Central Hikurangi Block (cf. Table 2). The uplift is detected at the GPS sites in the upper Raukumara Block.

5.1.1. Vertical rates in the Central Volcanic Zone

The largest localized vertical motions are detected throughout the Central Volcanic Zone. The maximum ascending rate there is 9.8 mm/yr (GPS site RGMT) in the Bay of Plenty region. The uplift in this region is also detected at the GPS sites RGOP (1.8 mm/yr) and TRNG (0.4 mm/yr). The maximum subsidence is found in the Rotorua region at a rate of 17.0 mm/yr (GPS site RGMK). The subsidence is also detected at the GPS sites RGKA (0.9 mm/yr) and RGTA (13.0 mm/yr). In the Taupo region, the localized uplift is detected at the GPS sites TGRA (0.5 mm/yr) and TAUP

Table 2. Classification of vertical crustal motions at GPS sites with respects to tectonic block configuration (as shown in Fig. 1) for the North Island (top) and the South Island (bottom). Note that the central and lower parts of the Raukumara Block, Central Hikurangi Block and Axial Ranges Block are located along the Dextral Fault Belt of the North Island. On the South Island the Marlborough Fault Zone comprises the North Canterbury Block, Seaward Kaikoura Block, Cloudy Bay Block and Inland Kaikoura Block.

Tectonic block		**GPS sites**	**Rates** [mm/yr]	**Motion**
(CEFZ) Cape Egmont Fault Zone and upper North Island		MAHO, HAMT, CORM, TAKL, AUCK	0.2–1.9	subsidence
(WANG) upper **Wanganui Block**		NPLY, WANG, GNBK	0.3–3.1	subsidence
(TVZ) Taupo Volcanic Zone		VGPK, VGTR, VGWH, VGTS, VGFW, VGOB, VGOT, VGKR, TGHR, TGWH, TGTK, RGHR, RGRR, RGTA, RGUT, RGMK, RGCR, RGRE, RGKA, RGLI	0.0–17.0	subsidence
		VGMT, VGMO, VGWN, TGRA, TAUP, RGMT, RGOP, TRNG	0.4–9.8	uplift
(RAUK) Raukumara Block	upper	MATW, CNST, PUKE, HIKB	0.1–1.5	uplift
	central and lower	GISB, HANA, PARI, KOKO, MARI, RAHI, NMAI, LEYL, MCNL, HAST, WPAW, WPUK, DNVK, HOLD	0.0–7.3	subsidence
(CHIK) Central Hikurangi Block		TINT, BIRF, PTOI, AKTO, PORA, PAWA, KAHU, CKD	0.3–5.7	subsidence
(AXIA) Axial Ranges Block		WGTN, WGTT, GRAC, AVLN, CLM, PEAK, KAPT, OTAK, LEVN, MANG, KORO, NRRD, MTBL, GRNR, TAKP, PNUI, KERE, UTK2, UTK3, UTK4, THAP, BHST, RIPA, TGOH, RGAR	0.0–9.3	subsidence
(WAIR) Wairarapa Block		PALI, PARW, TRAV, TEMA, MAST, CAST	3.3–4.9	subsidence

Tectonic block		**Continuous GPS sites**	**Rates** [mm/yr]	**Motion**
(SOUT) Southern Block		BLUF, LEXA	0.0–0.1	subsidence
(FIOR) Fiordland Block		PYGR, MAVL, HAAS	0.2–1.0	uplift
(CANT) Canterbury/Otago Block		DUNT, DUND, OUSD, WAM, LYTT, MQZG	0.1–1.4	subsidence
(SAB) Southern Alps Block		HOKI, QUAR, KARA, WAKA, CNCL, NETT, HORN, BNET, MTJO	0.2–4.5	uplift
(BRF) Buller Region Faults including **(WANG)** lower **Wanganui Block**		WEST, GLDB, NLSN, DURV	1.4–1.5	subsidence
(NCAN) North Canterbury Block	west	LKTA	1.2	uplift
	east	KAK	1.3	subsidence
(SKAI) Seaward Kaikoura Block		CMBL	0.0	No motion
(CBAY) Cloudy Bay Block		TORY	0.0	No motion
(IKAI) Inland Kaikoura Block		No data		

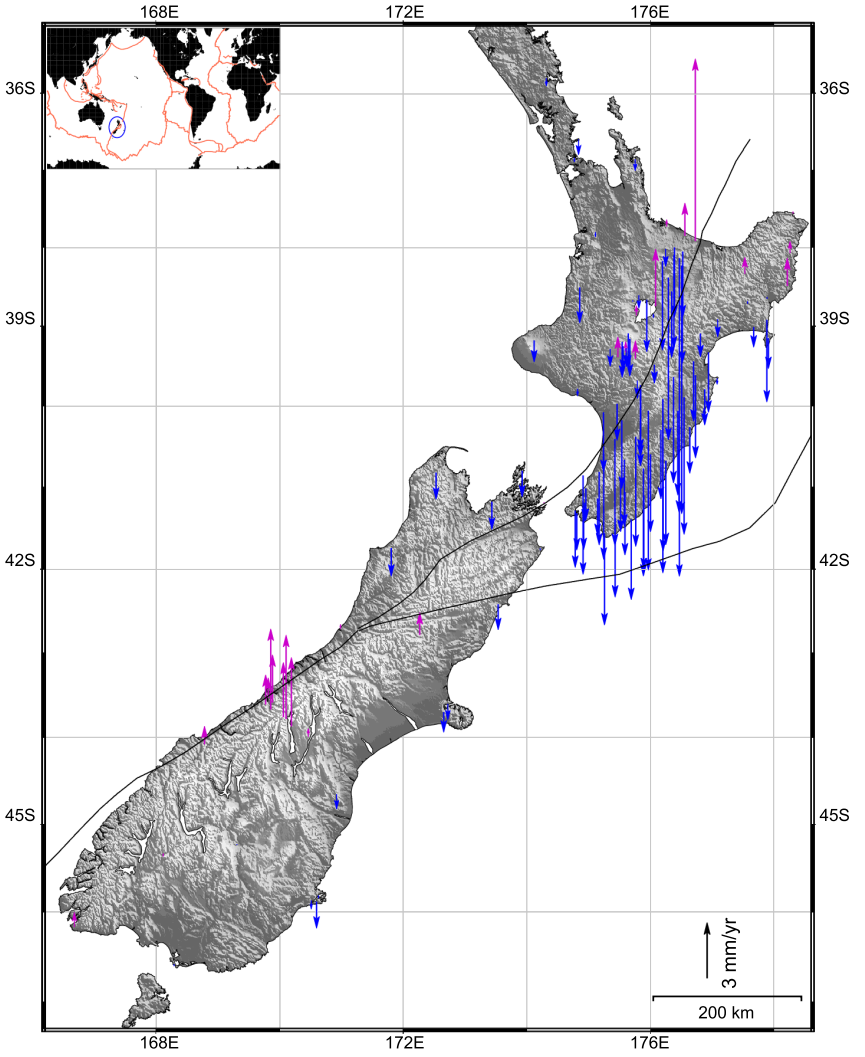

Fig. 2. Vertical velocity rates [mm/yr] at 123 GPS sites in New Zealand aligned to the ITRF2008 reference frame.

(3.1 mm/yr). In contrast, the subsidence is detected at the GPS sites TGOH (0.2 mm/yr), TGWH (2.7 mm/yr) and TGTG (0.6 mm/yr), while TGHR shows no vertical motion. Similar rates of subsidence of 1.9 and 1.8 mm/yr are seen at the GPS sites VGOT and VGKR located close to the Ton-

gariro Volcanic Group and Ngauruhoe volcano. The complex pattern of vertical motions is found at the Ruapehu active volcanic area. The GPS sites (VGMT, VGWN, VGMO) on the southern slopes show the uplift between 0.6–1.1 mm/yr. The northern GPS sites show the rate of subsidence between 0.9 mm/yr (GPS site VGPK) and 1.9 mm/yr (GPS site VGOB).

5.2. South Island vertical motions

As seen in Fig. 2, the vertical motions in the South Island are characterized by the tectonic uplift of the Southern Alps (west North Canterbury Block, Southern Alps Block and Fiordland Block) coupled by the subsidence detected at GPS sites located in the Buller Region (including the lower Wanganui Block), eastern North Canterbury Block, Canterbury/Otago Block, Southland Block including tectonic blocks which form the Marlborough Fault System (cf. Table 2).

5.2.1. Southern Alps Block

The comparison of vertical rates aligned to the ITRF2008 reference frame with the (relative) rates estimated by *Beavan et al. (2010)* at the continuous GPS sites (HOKI, QUAR, KARA, WAKA, CNCL, NETT, HORN, BNET, MTJO) across the Southern Alps is shown in Fig. 3. Both solutions show that the largest uplift across this profile corresponds typically with the highest topography while gradually decreasing towards the foothills on both sides of the profile. The largest disagreement (of $\sim$1 mm/yr) between these two solutions is at the GPS sites QUAR and HORN. From our results the maximum uplift detected across the Southern Alps is 4.5 mm/yr (GPS site HORN).

6. Summary and concluding remarks

We have investigated the vertical tectonic deformations in New Zealand using the GPS data provided by the GeoNET project. The GPS time series were processed in the PPP mode of GIPSY-OASIS II software and using the JPL reprocessed products.

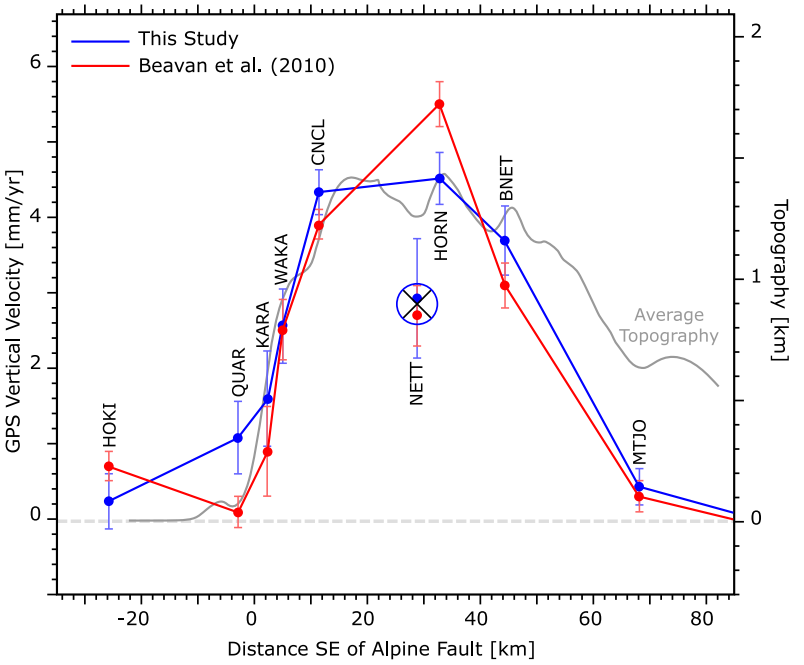

Fig. 3. Comparison of the vertical velocity rates (aligned to the ITRF2008 reference frame) with results by *Beavan et al. (2010)* on the study profile across the Southern Alps. The error bars define 95% confidence limits. Solid grey line shows smoothed topography along transect.

The results reveal that the upper North Island is tectonically relatively stable with the subsidence typically less than 1 mm/yr. This subsidence increases gradually along the western coastal regions. Despite the tectonic subsidence prevailing over most of the North Island, localized uplift has been detected at some GPS sites in the Taupo Volcanic Centre and Taupo Fault Belt. These regions are characterized by the largest detected vertical displacements in New Zealand within −17 mm/yr (GPS site RGMK) and 10 mm/yr (GPS site RGMT). The prevailing subsidence there is attributed to the back-arc rifting of the Taupo Volcanic Zone, with more localized vertical motions due to tectonism, active volcanism and geothermal processes. The uplift is also detected at the GPS sites situated on the eastern North Island, with the velocity rates typically less than 1 mm/yr. This uplift is probably explained by the crustal shortening (cf. *Barnes and Mercier*

de Lepinay, 1997; Nicol et al., 2002; Nicol and Beavan, 2003). The most prominent tectonic feature seen on the North Island is the systematic subsidence (with the maximum vertical displacements up to ∼9 mm/yr) detected throughout the Dextral Fault Belt. This subsidence is caused by the oceanic subduction of the Pacific oceanic plate underneath the Australian continental plate along the Hikurangi Trough.

The regional vertical tectonism of the South Island can be characterized by the uplift of the Southern Alps coupled on both sides by the systematic subsidence. The largest detected vertical rates of the tectonic uplift are found in the central Southern Alps at the current maximum rate of 4.5 mm/yr. This value is slightly smaller than the relative vertical rates estimated by *Beavan et al. (2004; 2010)* and *Tenzer et al. (2012)*. This rate is also significantly smaller than the values estimated by *Wellman (1979)*. He used geochronological data to compile a map of vertical tectonic deformations for the whole of the South Island. From his results, the maximum uplift along the Southern Alps reaches ∼10 mm/yr. According to his estimates, the velocity rates between 1 and 7 mm/year along the Alpine Fault further decrease to less than 1 mm/year in the south-east and north-west parts of the South Island. The uplift rates estimated by *Wellman (1979)* throughout the Southern Alps agree with more recent estimates from the geochronological data by *Tippet and Kamp (1993)*, but are about two times larger than the results from the GPS time series. Elsewhere in the South Island the vertical velocity rates at GPS sites estimated in this study indicate the systematic subsidence, while the results from the geochronological data (*Wellman, 1979; Tippet and Kamp, 1993*) indicate the presence of slight uplift. The systematic subsidence of the Buller Region in the northwest South Island) is detected at a rate of 1.4–1.5 mm/yr. The detected subsidence of the eastern South Island is smaller with the vertical rates typically less than 10 mm/yr. We note here that a more detailed comparison is still restricted by the currently low spatial coverage of GPS sites at the South Island.

The classification of vertical motions with respect to the tectonic block configuration in New Zealand revealed that most of the tectonic blocks are systematically either uplifted/subducted or tilted, except for the Taupo Volcanic Zone, which has a complex pattern of vertical motions with localized uplift and subsidence. On the North Island, the GPS sites situated at the Cape Egmont Fault Zone, (upper) Wanganui Block, Central Hiku-

rangi Block, Axial Ranges Block and Wairarapa Blocks shows a systematic subsidence. The tectonic tilting is detected in the Raukumara Block with its northern part uplifted, stable central part and subsiding southern part. On the South Island, the tilting is also observed in the North Canterbury Block, with the detected uplift of its western part (located in the vicinity of the Southern Alps) coupled by the subsidence of its eastern part. The Fiordland Block and Southern Alps Block are systematically uplifted. The Southern Block and Buller Region Faults (including the lower Wanganui Block) are subsiding, while the Seaward Kaikoura Block and Cloudy Bay Block are apparently stable.

These results indicate that the vertical motion of each tectonic block could be relatively closely described by the parameters of tilting. In this way, we can define the 3-D tectonic model of each block with the parameters of rotation (i.e. horizontal component) and tilting (vertical component). In most cases, this description could be further simplified by using only the parameter of vertical uplift/subsidence.

Acknowledgements. We thank CalTech/JPL for providing the GIPSY-OASIS II. We acknowledge the New Zealand GeoNet project and its sponsors EQC, GNS Science and LINZ, for providing GPS data used in this study. Figures were produced using Generic Mapping Tools (*Wessel and Smith, 1995*).

References

Altamimi Z., Collilieux X., Metivier L., 2011: ITRF2008: an improved solution of the international terrestrial reference frame. J. Geod., **85**, 5, 457–473, doi: 10.1007/s00190-011-0444-4.

Amiri-Simkooei A. R., Tiberius C. C. J. M., Teunissen P. J. G., 2007: Assessment of noise in GPS coordinate time series: methodology and results. J. Geophys. Res., **112**, B07413, doi: 10.1029/2006JB004913.

Barnes P. M., Mercier de Lepinay B., 1997: Rates and mechanics of rapid frontal accretion along the very obliquely convergent southern Hikurangi margin, New Zealand. J. Geophys. Res., **102**, B11, 24931–24952, doi: 10.1029/97JB01384.

Bar-Sever Y. E., Kroger P. M., Borjesson J. A., 1998: Estimating horizontal gradients of tropospheric path delay with a single GPS receiver. J. Geophys. Res, **103**, B3, 5019–5035.

Batt G. E., Braun J., 1999: The tectonic evolution of the Southern Alps, New Zealand: insights from fully thermally coupled dynamical modelling. Geophys. J. Int. **136**, 2, 403–420, doi: 10.1046/j.1365-246X.1999.00730.x.

Beanland S., 1995: The North Island dextral fault belt, Hikurangi subduction margin, New Zealand. Unpublished PhD thesis, Victoria Univ. of Wellington, Wellington, New Zealand.

Beanland S., Haines J., 1998: The kinematics of active deformation in the North Island, New Zealand, determined from geological strain rates. N.Z. J. Geol. Geophys., **41**, 4, 311–323, doi: 10.1080/00288306.1998.9514813.

Beavan J., Moore M., Pearson C., Henderson M., Parsons B., Bourne S., England P., Walcott D., Blick G., Darby D., Hodgkinson K., 1999: Crustal deformation during 1994–1998 due to oblique continental collision in the central Southern Alps, New Zealand, and implications for seismic potential of the Alpine Fault. J. Geophys. Res., **104**, B11, 25233–25255, doi: 10.1029/1999JB900198.

Beavan J., Haines J., 2001: Contemporary horizontal velocity and strain rate fields of the Pacific-Australian plate boundary zone through New Zealand. J. Geophys. Res., **106**, B1, 741–770, doi: 10.1029/2000JB900302.

Beavan J., Tregoning P., Bevis M., Kato T., Meertens C., 2002: Motion and rigidity of the Pacific Plate and implications for plate boundary deformation. J. Geophys. Res., **107**, B10, ETG19-1–ETG19-15, doi: 10.1029/2001JB000282.

Beavan J., Matheson D., Denys P., Denham M., Herring T., Hager B., Molnar P., 2004: A vertical deformation profile across the Southern Alps, New Zealand, from 3.5 years of continuous GPS data. In: Proceedings of Workshop, The State of GPS Vertical Positioning Precision: Separation of Earth Processes by Space Geodesy, Cahiers du Centre Européen de Geodynamique et de Sismologie, **23**, (Eds) van Dam T., Francis O., 111–123, Luxembourg, 2004.

Beavan J., Blick G., 2005: Limitations in the NZGD2000 Deformation Model. In: Dynamic Planet, International Association of Geodesy Symposia, 624–630, doi: 10.1007/978-3-540-49350-1_90.

Beavan J., 2005: Noise properties of continuous GPS data from concrete pillar geodetic monuments in New Zealand and comparison with data from US deep drilled braced monuments. J. Geophys. Res., **110**, B08410, doi: 10.1029/2005JB003642.

Beavan J., Ellis S., Wallace L., Denys P., 2007: Kinematic constraints from GPS on oblique convergence of the Pacific and Australian Plates, central South Island, New Zealand. In: A Continental Plate Boundary: Tectonics at South Island, New Zealand, Okaya D., Stern T., Davey F. (Eds), Geophys. Monogr. Ser., **175**, 75–94, AGU, Washington DC, doi: 10.1029/175GM05.

Beavan J., Denys P., Denham M., Hager B., Herring T., Molnar P., 2010: Distribution of present-day vertical deformation across the Southern Alps, New Zealand, from 10 years of GPS data. Geophys. Res. Lett., **37**, L16305, doi: 10.1029/2010GL044165.

Berryman K. R., Beanland S., Cooper A. F., Cutten H. N., Norris R. J., Wood P. R., 1992: The Alpine Fault, New Zealand; variation in Quaternary structural style and geomorphic expression. Ann. Tectonicae (Supplement), **6**, 126–163.

Blick G., Crook C., Grant D., Beavan J., 2003: Implementation of a semi-dynamic datum for New Zealand. In: Sanso F. (Ed.) A Window on the Future of Geodesy. Springer-Verlag, Berlin/Heidelberg, 38–43, doi: 10.1007/3-540-27432-4_7.

Boehm J., Niell A. E., Tregoning P., Schuh H., 2006: The Global Mapping Function (GMF): A new empirical mapping function based on numerical weather model data. Geophys. Res. Lett., **33**, 7, L07304, doi: 10.1029/2005GL025546.

Bourne S. J., Arnadottir T., Beavan J., Darby D. J., England P. C., Parsons B., Walcott R. I., Wood P. R., 1998: Crustal deformation of the Marlborough fault zone in the South Island of New Zealand: Geodetic constraints over the interval 1982–1994. J. Geophys. Res., **103**, B12, 30147–30165, doi: 10.1029/98JB02228.

Bull W. A., Cooper A. F., 1986: Uplifted marine terraces along the Alpine Fault, New Zealand. Science **234**, 4781, 1225–1228, doi: 10.1126/science.234.4781.1225.

Cande S. C., Stock J. M., 2004: Pacific-Antarctic-Australia motion and the formation of the Macquarie Plate. Geophys. J. Int., **157**, 1, 399–414, doi: 10.1111/j.1365-246X.2004.02224.x.

Cole J. W., Darby D. J., Stern T. A., 1995: Taupo Volcanic Zone and Central Volcanic Region Backarc Structures of North Island, New Zealand. In: Taylor B. (Ed.), Backarc Basins. Springer US, Boston, MA, 1–28.

Dach R., Hugentobler U., Fridez P., Meindl M., 2007: Bernese GPS Software Version 5.0., p. 612, Astron. Inst., Univ. of Bern, Bern.

DeMets C., Gordon R. G., Argus D. F., Stein S., 1990: Current plate motions. Geophys. J. Int., **101**, 2, 425–478, doi: 10.1111/j.1365-246X.1990.tb06579.x.

DeMets C., Gordon R. G., Argus D. F., Stein S., 1994: Effect of recent revisions to the geomagnetic reversal timescale on estimates of current plate motions. Geophys. Res. Lett., **21**, 20, 2191–2194, doi: 10.1029/94GL02118.

DeMets C., Gordon R. G., Argus D. F., 2010: Geologically current plate motions. Geophys. J. Int., **181**, 1, 1–80, doi: 10.1111/j.1365-246X.2009.04491.x.

Grindley G. W., Hull A. G., 1986: Historical Taupo earthquakes and earth deformation. R. Soc. N.Z. Bull., **24**, 173–186.

Holt W. E., Haines A. J., 1995: The kinematics of northern South Island, New Zealand, determined from geologic strain rates. J. Geophys. Res., **100**, B9, 17991–18010, doi: 10.1029/95JB01059.

Herring T. A., 2003: Matlab Tools for viewing GPS velocities and time series. GPS solutions, **7**, 3, 194–199.

Kelsey H. M., Cashman S. M., Beanland S., Berryman K. R., 1995: Structural evolution along the inner forearc of the obliquely convergent Hikurangi margin, New Zealand. Tectonics, **14**, 1, 1–18, doi: 10.1029/94TC01506.

Kim M. J., Schwartz S. Y., Bannister S., 2011: Non-volcanic tremor associated with the March 2010 Gisborne slow slip event at the Hikurangi subduction margin, New Zealand. Geophys. Res. Lett., **38**, L14301, doi:10.1029/2011GL048400.

Langbein J., Johnson H., 1997: Correlated errors in geodetic time series: implications for time dependent deformation. J. Geophys. Res., **102**, B1, 591–603, doi: 10.1029/96JB02945.

Lyard F., Lefevre F., Letellier T., Francis O., 2006: Modelling the global ocean tides: modern insights from FES2004. Ocean Dyn., **56**, 5, 394–415, doi: 10.1007/s10236-006-0086-x.

Mao A., Harrison C. G. A., Dixon T. H., 1999: Noise in GPS coordinate time series. J. Geophys. Res., **104**, B2, 2797–2816, doi: 10.1029/1998JB900033.

Nicol A., Van Dissen R. J., Vella P., Alloway B. V., Melhuish A., 2002: Growth of contractional structures during the last 10 m.y. at the southern end of the emergent Hikurangi forearc basin, New Zealand. N.Z. J. Geol. Geophys., **45**, 3, 365–385, doi: 10.1080/00288306.2002.9514979.

Nicol A., Beavan J., 2003: Shortening of an overriding plate and its implications for slip on a subduction thrust, central Hikurangi Margin, New Zealand. Tectonics, **22**, 6, 1070, doi: 10.1029/2003TC001521.

Nicol A., Mazengarb C., Chanier F., Rait G., Uruski C., Wallace L. M., 2007: Tectonic evolution of the active Hikurangi subduction margin, New Zealand, since the Oligocene. Tectonics, **26**, 4, TC4002, doi: 10.1029/2006TC002090.

Nicol A., Wallace L. M., 2007: Temporal stability of deformation rates: comparison of geological and geodetic observations, Hikurangi Subduction Margin, New Zealand. Earth Planet Sci. Lett., **258**, 3-4, 397–413, doi: 10.1016/j.epsl.2007.03.039.

Norris R. J., Cooper A. F., 2001: Late Quaternary slip rates and slip partitioning on the Alpine Fault, New Zealand. J. Struct. Geol., **23**, 2-3, 507–520, doi: 10.1016/S0191-8141(00)00122-X.

Otway P. M., 1986: Vertical deformation associated with the Taupo earthquake swarm, June 1983. In: Reilly W. I., Harford B. E. (Ed.): Recent crustal movements of the Pacific region, Wellington, R. Soc. N.Z. Bull., **24**, 187–200.

Otway P. M., Blick G. H., Scott B. J., 2002: Vertical deformation at Lake Taupo, New Zealand, from lake levelling surveys, 1979–1999. N.Z. J. Geol. Geophys., **45**, 1, 121–132, doi: 10.1080/00288306.2002.9514964.

Petit G., Luzum B., Eds., 2010: IERS conventions (2010), IERS Tech Note 36, Bundesamts für Kartogr. und Geod., Frankfurt am Main, Germany, p. 179, ISBN 3-89888-989-6.

Samsonov S., Beavan J., Gonzalez P. J., Tiampo K., Fernandez J., 2011: Ground deformation in the Taupo Volcanic Zone, New Zealand, observed by ALOS PALSAR interferometry. Geophys. J. Int., **187**, 1, 147–160, doi: 10.1111/j.1365-246X.2011.05129.x.

Schmid R., Steigenberger P., Gendt G., Ge M., Rothacher M., 2007: Generation of a consistent absolute phase center correction model for GPS receiver and satellite antennas. J. Geod., **81**, 12, 781–798, doi: 10.1007/s00190-007-0148-y.

Sutherland R., Norris R. J., 1995: Late Quaternary displacement rate, paleoseismicity, and geomorphic evolution of the Alpine Fault; evidence from Hokuri Creek, South Westland, New Zealand. N.Z. J. Geol. Geophys., **38**, 4, 419–430, doi: 10.1080/00288306.1995.9514669.

Tenzer R., Stevenson M., Denys P., 2012: A Compilation of a Preliminary Map of Vertical Deformations in New Zealand from Continuous GPS Data. In: Kenyon S., Pacino M. C., Marti U. (Eds), Geodesy for Planet Earth. Springer Berlin Heidelberg, Berlin, Heidelberg, 697–703, doi: 10.1007/978-3-642-20338-1_86.

Tippett J. M., Kamp P. J. J., 1993: Fission track analysis of the late Cenozoic vertical kinematics of continental Pacific Crust, South Island, New Zealand. J. Geophys. Res., **98**, B9, 16119–16148, doi: 10.1029/92JB02115.

Villamor P., Berryman K. R., 2001: A Late Quaternary extension rate in the Taupo Volcanic Zone, New Zealand, derived from fault slip data. N.Z. J. Geol. Geophys., **44**, 2, 243–269, doi: 10.1080/00288306.2001.9514937.

Walcott R. I., 1984: The kinematics of the plate boundary zone through New Zealand: a comparison of short-and long-term deformations. Geophys. J. R. Astr. Soc., **79**, 2, 613–633, doi: 10.1111/j.1365-246X.1984.tb02244.x.

Wallace L. M., Beavan J., McCaffrey R., Darby D., 2004: Subduction zone coupling and tectonic block rotations in the North Island, New Zealand. J. Geophys. Res., **109**, B12406, doi: 10.1029/2004JB003241.

Wallace L. M., Beavan J., McCaffrey R., Berryman K., Denys P., 2007: Balancing the plate motion budget in the South Island, New Zealand using GPS, geological and seismological data. Geophys. J. Int., **168**, 1, 332–352, doi: 10.1111/j.1365-246X.2006.03183.x.

Wallace L. M., Beavan J., 2010: Diverse slow slip behavior at the Hikurangi subduction margin, New Zealand. J. Geophys. Res., **115**, B12402, doi: 10.1029/2010JB007717.

Wdowinski S., Bock Y., Zhang J., Fang P., Genrich J. F., 1997: Southern California Permanent GPS Geodetic Array: Spatial filtering of daily positions for estimating coseismic and postseismic displacements induced by the 1992 Landers earthquake. J. Geophys. Res., **102**, B8, 18057–18070, doi: 10.1029/97JB01378.

Webb F. H., Zumberge J. F., 1995: An introduction to GIPSY-OASIS-II precision software from the analysis of data from the Global Positioning System. Report, JPL D-11088, Pasadena, California Institute of Technology.

Wellman H. W. 1979: An uplift map for the South Island of New Zealand, and a model for uplift of the Southern Alps. R. Soc. N.Z. Bull., **18**, 13–20.

Wessel P., Smith W. H. F., 1995: New version of generic mapping tools released. EOS Trans. Am. Geophys. Union, **76**, p. 329.

Williams S. D. P, 2003: The effect of coloured noise on the uncertainties of rates estimated from geodetic time series. J. Geod., **76**, 9, 483–494, doi: 10.1007/s00190-002-0283-4.

Williams S. D. P., 2008: CATS: GPS coordinate time series analysis software. GPS Solutions, **12**, 2, 147–153, doi: 10.1007/s10291-007rr0086-4.

Zumberge J. F., Heflin M. B., Jefferson D. C., Watkins M. M., Webb F. H., 1997: Precise Point Positioning for the efficient and robust analysis of GPS data from large networks. J. Geophys. Res., **102**, B3, 5005–5017, doi: 10.1029/96JB03860.